Deep ultraviolet emission in hexagonal boron nitride grown by high-temperature molecular beam epitaxy

2017 2D Mater. 4 021023

(http://iopscience.iop.org/2053-1583/4/2/021023)

2D Materials

OPEN ACCESS

RECEIVED
19 December 2016

REVISED
3 February 2017

ACCEPTED FOR PUBLICATION
10 February 2017

PUBLISHED
17 March 2017

LETTER

Deep ultraviolet emission in hexagonal boron nitride grown by high-temperature molecular beam epitaxy

T Q P Vuong[1], G Cassabois[1], P Valvin[1], E Rousseau[1], A Summerfield[2], C J Mellor[2], Y Cho[2], T S Cheng[2], J D Albar[2], L Eaves[2], C T Foxon[2], P H Beton[2], S V Novikov[2] and B Gil[1]

[1] Laboratoire Charles Coulomb, UMR5221 CNRS-Université de Montpellier, 34095 Montpellier, France
[2] School of Physics and Astronomy, University of Nottingham, Nottingham NG7 2RD, United Kingdom

E-mail: guillaume.cassabois@umontpellier.fr

Keywords: boron nitride, molecular beam epitaxy, deep ultraviolet

Abstract

We investigate the opto-electronic properties of hexagonal boron nitride grown by high temperature plasma-assisted molecular beam epitaxy. We combine atomic force microscopy, spectroscopic ellipsometry, and photoluminescence spectroscopy in the deep ultraviolet to compare the quality of hexagonal boron nitride grown either on sapphire or highly oriented pyrolytic graphite. For both substrates, the emission spectra peak at 235 nm, indicating the high optical quality of hexagonal boron nitride grown by molecular beam epitaxy. The epilayers on highly oriented pyrolytic graphite demonstrate superior performance in the deep ultraviolet (down to 210 nm) compared to those on sapphire. These results reveal the potential of molecular beam epitaxy for the growth of hexagonal boron nitride on graphene, and more generally, for fabricating van der Waals heterostructures and devices by means of a scalable technology.

1. Introduction

At present there is a great interest in the potential of van der Waals (vdW) heterostructures as a new platform for two-dimensional (2D) devices [1]. Exfoliation methods using adhesive tape techniques have been used extensively to produce the first 2D materials such as graphene, hexagonal boron nitride (hBN) and the transition metal dichalcogenides, with typical planar dimensions of a few tens of micrometres [2]. Such methods have enabled the fabrication of monolayer-thick graphene and multilayer vdW devices [1]. However, these methods are difficult, time-consuming and are not scalable. Therefore, the development of an alternative scalable growth technology is urgently required for 2D materials and devices. It is well known from decades of previous research in semiconductor physics and technology, that epitaxy is the most appropriate technical approach to produce large area devices at moderate cost. The development of scalable epitaxial growth methods for 2D vdW heterostructures is essential to move the production of these materials from the research laboratory into the marketplace.

It is also important to recall that crystal growers have already demonstrated that 2D sacrificial buffer layers can be used to detach advanced III–V epitaxial opto-electronic devices from the expensive substrate used for growth [3]. This is particularly important for short wavelength light emitters based on the utilization of wurtzite nitrides, including GaN, AlN and their alloys, where no bulk lattice-matched substrates are available. The development of large-scale epitaxial growth of high quality hBN by both metal organic chemical vapour deposition (MOCVD), and, as shown here using high temperature molecular beam epitaxy (MBE), will be crucial for both of the above applications.

To obtain hBN of high crystalline quality it is essential to avoid transfer of defects into the active layers of a wurtzite epitaxial structure; these defects would be extremely detrimental in terms of performance. As-grown p-type hBN can be used as an efficient hole injector with the potential to replace the highly defective Mg-doped AlGaN layers in future device structures [4]. The quality of such p-type AlGaN-based hole injectors is currently low due to the high activation energy of Mg. The high Mg concentrations in the material that are required to achieve high hole densities in the valence band generate defects that absorb the emitted ultraviolet light and contribute to the collapse of the external quantum efficiency in existing deep ultraviolet devices [5]. The huge potential market for optoelectronic devices operating in the deep ultraviolet further highlights the need for high quality hBN.

The epitaxial growth of hBN by MOCVD has been demonstrated using different substrates such as sapphire (Al_2O_3) [6, 7], transition metal [8], copper [9], amorphous SiO_2 and quartz [10]. High temperature growth conditions are beneficial for the growth of hBN, and sapphire is a convenient substrate. However, during the initial stages of hBN growth on sapphire [6], it is difficult to avoid the formation of AlN at the interface due to nitridation of the sapphire substrate by active nitrogen. The band gaps of hBN and AlN are similar and therefore the formation of AlN will complicate the interpretation of the optical properties of hBN. A further complication in the analysis of photoluminescence (PL) is the different nature of the band alignment in AlN and hBN. AlN is a direct bandgap semiconductor, leading to an efficient direct recombination. In contrast, hBN is an indirect bandgap semiconductor [11] so that strong luminescence features are not necessarily a signature of high quality hBN. In this material, one has to consider the interplay between the intrinsic phonon-assisted recombination and the extrinsic defect-mediated emission processes.

In order to eliminate the influence of nitridation of sapphire on the quantitative analysis of the emission spectrum and therefore of the quality of our hBN epilayers, we have investigated the optical properties of hBN deposited not only on sapphire, but also on highly ordered pyrolytic graphite (HOPG) substrates. HOPG is not a standard MBE substrate, but is a good alternative to sapphire, because hBN is closely lattice-matched to HOPG with a low lattice mismatch of ∼1.8%. Growth of hBN on HOPG is important for 2D device applications as a step towards development of graphene-boron nitride vdW heterostructures and devices.

2. Experiments

All of the hBN layers presented in this work were grown by high temperature MBE at substrate temperatures between 1200 and 1700 °C (thermocouple temperatures). The MBE system is a dual-chamber Veeco GENXplor specially modified to achieve growth temperatures of up to 1850 °C and is capable of growth on rotated substrates of up to 3 inches in diameter. In MBE, the substrate temperature is normally measured using an optical pyrometer. Because we use transparent sapphire substrates, the pyrometer measures the temperature of the substrate heater, not the substrate surface. Therefore, our estimate of the growth temperature is based on a thermocouple reading. A high-temperature solid-source effusion cell was used for boron and a Veeco radio-frequency (RF) plasma source to produce an active nitrogen flux. Details of the MBE system are described elsewhere [12–14]. The hBN layers were all grown using a boron cell temperature of 1875 °C and the nitrogen source operated at 550 W with a nitrogen flow rate of 2 sccm.

Two types of $10 \times 10\,mm^2$ substrates were used for the MBE growth: sapphire (0 0 0 1) and HOPG (mosaic spread 0.4°). Before introduction into the MBE growth chamber the HOPG substrates were cleaned by exfoliation using adhesive tape to obtain a fresh surface for growth. Following exfoliation, substrates were further cleaned by immersion in toluene (CHROMASOLV for HPLC, Sigma-Aldrich) for 24 h and after that, thermally cleaned in a tube furnace at ∼200 °C in a flow of Ar:H_2 (95:5) gas (0.15 standard litres per minute for 4 h) to remove any remaining polymer residue.

The MBE-grown layers were studied by atomic force microscopy (AFM), spectroscopic ellipsometry, and PL spectroscopy. These measurements were all performed under ambient conditions, except for PL experiments at cryogenic temperatures.

For topographic imaging of the grown hBN layers, amplitude-modulated tapping (AC) mode atomic force microscopy (AC-AFM) was performed in ambient conditions using an Asylum Research Cypher-S AFM. Samples were imaged using MultiAl-75G (Budget Sensors, stiffness ∼3 N m^{-1}) AFM cantilevers in repulsive mode, with the exception of the AFM image in figure 2(a) which was acquired in contact mode.

Variable angle spectroscopic ellipsometry was carried out using a M2000-DI instrument made by J.A. Woollam Inc. The results were obtained over a wavelength range from 1690 to 192 nm using focussing probes resulting in an elliptical spot with a minor axis of 200 μm, the major axis of the ellipse depends on the angles of incidence used which were 55°, 60° and 65°. Analysis was carried out using CompleteEase version 5.19.

In the PL studies the hBN samples were excited by the fourth harmonic of a cw mode-locked Ti:Sa oscillator with a repetition rate of 82 MHz. The spot diameter was of the order of 300 μm with an excitation power of 50 μW. An achromatic optical system couples the emitted signal to our detection system, where the PL signal is dispersed in a $f = 500$ mm Czerny–Turner monochromator, equipped with a 1800 grooves mm^{-1} grating blazed at 250 nm, and recorded with a back-illuminated CCD camera (Andor Newton 920), with a quantum efficiency of 50% at 210 nm, over integration times of 1 min.

3. Results and discussion

3.1. Atomic force microscopy

Figure 1 shows AFM images of two hBN samples after 3 h of MBE growth on a sapphire substrate. For these samples, a uniform nano-crystallite morphology with hBN nanocrystallites covering the entire sapphire surface is observed. This morphology is consistent for all growth temperatures in the range 1390–1690 °C, with the exception of the highest growth temperature sample (1690 °C) as shown in figure 1(b), in which the underlying terraces of the sapphire substrate are visible through the hBN deposits. We attribute this to re-evaporation of hBN from the sapphire substrate at these high temperatures, resulting in a thinner hBN layer

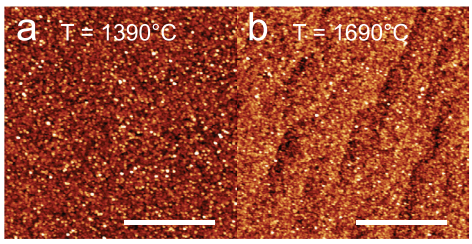

Figure 1. Atomic force microscopy images of two hBN samples grown on sapphire for 3 h, at 1390 °C (a), and 1690 °C (b). The AFM images were acquired using AC mode AFM, and the scale bars in both images are 2 μm.

that will allow the atomic corrugations of the atomic sapphire terraces to be distinguished in the topography. Estimations of the average hBN film thickness indicate indeed a monotonic decrease with the growth temperature, from ∼17 nm to ∼5 nm (table 1).

The morphology of the hBN epilayers grown on HOPG is markedly different to those grown on sapphire. AFM images of the hBN on HOPG surface are shown in figure 2 for growth temperatures from 1390–1690 °C. In agreement with our previously reported work [14], we observe faceted hBN islands nucleating from HOPG step edges, and bulk hBN deposits. The hBN islands form a near-complete monolayer for the lowest growth temperature as shown in figure 2(a) (1390 °C), together with multi-layered regions. Defects and grain boundaries are also observed on the hBN which indicate a laterally polycrystalline hBN surface. These conclusions are supported by scanning tunnelling microscopy measurements of different MBE hBN domains (not shown here). These samples exhibit moiré patterns of various sizes in the scans of tunnel current, which indicate a rotational mismatch between the hBN and HOPG lattices; these results will be reported elsewhere. The coverage of the hBN layer is strongly dependent on substrate temperature, as shown by the reduction in surface coverage with increasing temperature, due to hBN re-evaporation (figure 2). For the highest growth temperature presented in figure 2(d) (1690 °C), only a small amount of step-flow growth is observed from the step edges of the HOPG substrate. Such a phenomenology results again in a monotonic decrease of the hBN film thickness as a function of the growth temperature, with significantly lower values than for the growth on sapphire, as summarized in table 1.

3.2. Spectroscopic ellipsometry

In figure 3(a), we show the optical absorption coefficient as a function of photon energy for the four hBN samples grown on sapphire substrates. The absorption coefficients were calculated from an optical model that was determined by fitting the spectroscopic ellipsometric measurements to a Kramers–Krönig consistent optical model of Gaussian oscillators. The use of focussing probes avoids any effect of the reflection of the probe light from the back surface of the sapphire wafer. The optical model for the substrate was verified by measuring a sapphire wafer as a control sample.

Table 1. Average film thickness of hBN, in units of monolayer (ML), after 3 h of growth as a function of growth temperature (top line), and substrate (left column). 1 ML = 0.33 nm. Thickness values smaller than one correspond to the surface coverage.

	1390 °C	1480 °C	1560 °C	1690 °C
Sapphire	53 ± 3	40 ± 3	33 ± 3	15 ± 3
HOPG	1.15 ± 0.01	0.85 ± 0.01	0.38 ± 0.01	0.09 ± 0.01

Due to the indirect nature of the bandgap, the absorption onset in hBN is blue-shifted by one phonon energy compared to the excitonic gap at 5.95 eV [11]. Moreover, because of the unusual configuration of the bandstructure in hBN, the optical response involves phonons with a finite group velocity, leading to phonon replicas displaying sharp resonances [11] instead of the standard broad bands expected from the mapping of the excitonic quasi-continuum in phonon-assisted optical processes [15]. This results in an absorption peak at around 6.02 eV, as measured in PL excitation spectroscopy in high-purity bulk hBN [16]. The absorption spectra in figure 3(a) show the same phenomenology, with slight variations of the absorption spectrum around 6 eV depending on growth conditions of each of the MBE layers. The higher two substrate temperatures result in steep absorption edges, together with low residual absorption below it. The samples grown at the lower temperatures, 1390 °C and 1480 °C, exhibit significant absorption at energies between 4 and 5.5 eV. We will see below that this correlates with a strong decrease of the PL signal intensity.

Figure 4(a) shows absorption coefficient spectra calculated from spectroscopic ellipsometric measurements made on hBN grown on HOPG, a polycrystalline material with the surface normal to the grains having an angular spread of a few degrees. For these samples the fact that the focussing probes increase the acceptance angle for the reflected light allows the light reflected from the HOPG polycrystals to be collected inspite of the angular spread around the surface normal. The optical model of the substrate was verified by measuring the back of the sample. The optical response of the hBN was modelled in a similar manner to the samples grown on sapphire.

For the hBN grown on HOPG at the lower growth temperatures, the sharp increase in absorption also indicates a bandgap at around 6 eV similar to that of high-quality bulk hBN. At the highest growth temperature the absorption spectrum displays a smoother increase above 5 eV, possibly arising from greater inhomogeneity due to the reduction in surface coverage with increasing temperature (figure 2 and table 1). The hBN films are found to have thicknesses in the nm range (measured as an average value over the measurement ellipse), significantly thinner than the hBN on sapphire samples, in agreement with our estimations by AFM (table 1). The

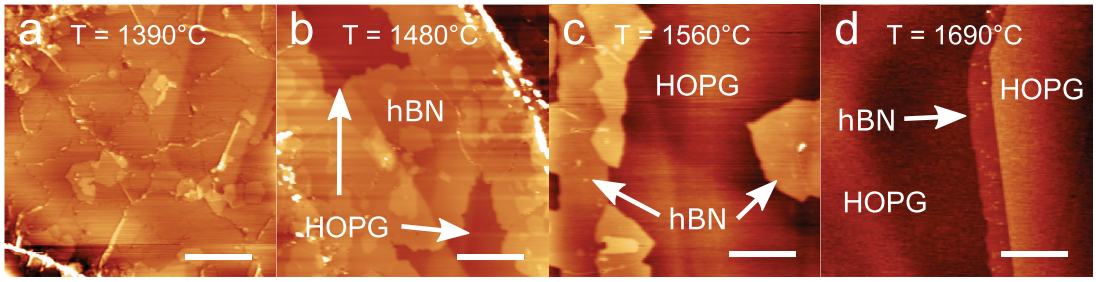

Figure 2. Atomic force microscopy images of hBN grown on HOPG for 3 h, at 1390 °C (a), 1480 °C (b), 1560 °C (c) and 1690 °C (d). The images show a gradual reduction in surface coverage from complete hBN coverage in (a) to island growth ((b) and (c)), and finally only growth from HOPG step-edges (d). The arrows in images ((b)–(d)) indicate the regions corresponding either to the underlying HOPG substrate (b), or to the hBN islands ((c) and (d)), following our comparative analysis detailed in [14]. The AFM images ((b)–(d)) were acquired using AC mode AFM, and image (a) was acquired in contact mode. The scale bars in images ((a)–(d)) are all 500 nm.

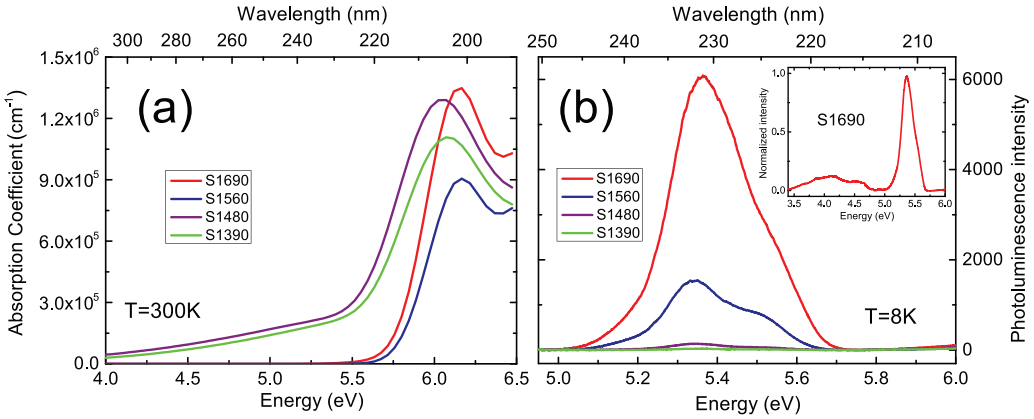

Figure 3. Absorption (a) and PL (b) spectra in the four hBN samples grown on sapphire, labelled with the substrate type (S = sapphire) followed by the growth temperature in °C. The absorption measurements were performed at 300 K, whereas the PL spectra were recorded at 8 K under excitation at 6.3 eV. Inset (b): PL spectrum of S1690 over a larger spectral range.

layers are so thin that there is limited confidence in the exact value, this may be the cause of the spread in the absolute magnitude of the absorption coefficient.

3.3. Photoluminescence

Figure 3(b) shows the PL spectra of the four hBN samples grown on sapphire substrates. Figure 4(b) shows the corresponding PL spectra for hBN samples grown on HOPG. In the two cases, we focus on the spectral range corresponding to the near band-edge emission of hBN, in the deep ultraviolet range between 5 and 6 eV [11, 17].

As shown in figure 3(b), we observe a strong dependence of the PL spectrum on growth substrate temperature for the samples. The most intense PL signal is recorded for the highest substrate temperature (1690 °C). The emission intensity demonstrates a monotonic decrease on reduction of the growth temperature, the PL signal intensity of the sample grown at lowest growth temperature (1390 °C) being approximately 200 times weaker than the highest. These variations are much larger than, and opposite to, the film thickness ones, which correspond to an increase by a factor of ~3 on reduction of the growth temperature for hBN on sapphire (see table 1), thus ruling out any excitation volume effect in the monotonic increase of the PL signal with growth temperature. Whereas the intensity of the PL spectrum is strongly temperature-dependent, the emission profile is almost identical in the four samples grown on sapphire. The PL spectrum maximum is at an energy of 5.36 eV with a secondary shoulder at a higher energy of ~5.55 eV. In our previous studies of PL from bulk hBN crystals synthesized by the NIMS high-temperature high-pressure (HTHP) growth method [17], two PL lines are present at 5.27 and 5.56 eV. These features were identified as arising from point defects as opposed to stacking faults [18]. This suggests the former type of defect is the origin of the emission lines reported here, which we further discuss below. Finally, we note that the decrease of the PL signal in the two lowest growth temperature samples is consistent with the appearance of a low-energy tail in the absorption spectra of these samples, around 4–5 eV as shown in figure 3(a). We interpret this effect as resulting from a higher density of deep levels in these samples, which open non-radiative recombination channels for the carriers that are photo-generated above the bandgap. For the layers grown on sapphire substrates, we thus infer a global improvement of the structural quality of hBN for increasing the temperature of the sapphire substrate.

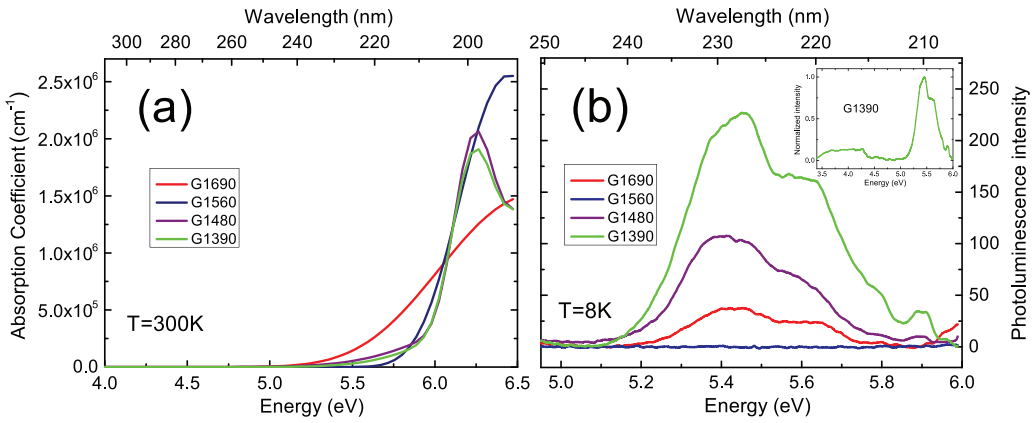

Figure 4. Absorption (a) and PL (b) spectra in the four hBN samples grown on highly-oriented pyrolitic graphite (HOPG), labelled with the substrate type (G = graphite) followed by the growth temperature in °C. The absorption measurements were performed at 300 K, whereas the PL spectra were recorded at 8 K under excitation at 6.3 eV. Inset (b): PL spectrum of G1390 over a larger spectral range.

We also observe a pronounced dependence of the PL spectrum on growth conditions for the hBN layers grown on HOPG substrates, as shown in figure 4(b). However, with HOPG substrates the evolution is reversed compared to the sapphire substrate samples, with the lowest substrate temperature (1390 °C) displaying the most intense and rich signal with additional lines at higher energy. However, we note that the dependence as a function of substrate temperature is not exactly monotonic, since the lowest PL signal is not recorded in the highest substrate temperature sample but in the second highest. In these two samples grown at the highest temperatures, the hBN coverage of the HOPG surface is drastically decreased because of hBN sublimation (figures2(c) and (d)), resulting in a non-uniform optical response. In fact, in figure 4(a), it was already noted that the absorption measurements around 6 eV in the two highest temperature samples (1560 and 1690 °C) were not very accurate because of the low hBN surface coverage. Conversely, in the sample grown at the lowest temperature on HOPG, we observed a bright emission up to 5.9 eV, which is characteristic of intrinsic phonon-assisted recombination in few monolayer-hBN samples of high-quality [19]. The presence of an emission line around 5.9 eV is a direct signature of the excellent crystalline quality of our hBN epilayers grown by high-temperature MBE, which will be further commented on below.

From the results of hBN grown on both sapphire and HOPG we conclude that the PL spectrum is dominated by an intense emission in the deep ultraviolet, centred around 5.4–5.5 eV with a full width at half maximum of the order of 300–400 meV. Similar to the pioneering paper by Watanabe *et al* on high-purity hBN single crystals [17], the bright emission in the deep ultraviolet in our hBN epilayers grown by MBE coincides with a low emission intensity from deep levels around 4 eV. This can be seen in the inset of figures 3(b) and 4(b) which display the PL spectrum over a wider spectral range from 3.5 to 6 eV. Therefore, high temperature MBE growth can produce hBN layers of high optical quality.

Although the PL spectra for hBN samples grown on sapphire and HOPG have strong similarities, the existence of an emission line around 5.9 eV in the two-lowest temperature samples grown on HOPG (figure 4(b)) is an extremely important observation as already pointed out above. This line is the fingerprint for recombination assisted by the emission of LA and TA phonons in hBN [11, 18, 20]. Since hBN is an indirect bandgap semiconductor, direct radiative recombination is forbidden because of momentum conservation. Light emission in hBN occurs via phonon-assisted processes, so that, in high-quality hBN crystals, the PL spectrum displays five lines at 5.76, 5.79, 5.86, 5.89, and 5.93 eV which were recently identified as phonon replicas, with an energy spacing reflecting the splitting of the different phonon branches (LO, TO, LA, TA, ZA, respectively) in the middle of the Brillouin zone [11, 18, 20]. Cathodoluminescence (CL) measurements in exfoliated hBN flakes of decreasing thickness also showed that the intensity ratio of the LO/TO and LA/TA phonon replicas reverses from bulk hBN down to few monolayer-samples [19]. Whereas the LO/TO phonon replica dominates the intrinsic emission spectrum in bulk hBN, the situation is opposite in few monolayer thick samples, where the PL spectrum is dominated by the LA/TA phonon replica. This is precisely what we observe in the lowest temperature hBN on HOPG samples shown in figure 4(b). The PL spectrum displays a pronounced line around 5.9 eV with a doublet structure at 5.88 and 5.91 eV, corresponding to the LA and TA phonon replicas, respectively (this doublet structure being more clearly resolved in [11]). The LO/TO phonon replica appears at 5.8 eV, as a high-energy shoulder of the dominant emission band centered around 5.4–5.5 eV. Following [19], the intensity ratio of the LO/TO and LA/TA phonon replicas of approximately 3 (after background correction in figure 4(b)) indicates an hBN-thickness of 2–3 nm in the lowest temperature hBN on HOPG sample, in agreement with our estimations from AFM measurements presented in figure 2 and summarized in table 1. Therefore, we conclude that the hBN films grown at the lowest growth temperature of

1390 °C using high-temperature MBE are high-quality epilayers with optical properties comparable to exfoliated hBN flakes. This advance in the synthesis of hBN by high-temperature MBE is even more noteworthy in comparison to MOCVD, which has been continuously improving for the last five years [6, 21], reaching an emission spectrum globally dominated by the 5.75 eV line [21], but never achieving optical properties comparable to thin exfoliated hBN flakes.

The PL spectrum of the 1390 °C sample also displays evidence of intervalley carrier scattering [18]. In high-quality hBN crystals synthesized by the HTHP growth method, it was demonstrated that the phonon cascade from the indirect exciton is not limited to one-phonon processes leading to the LO/TO and LA/TA phonon replicas, and that two-, three- and four-phonon-assisted recombination features appear at lower energy. More specifically, transverse optical phonons at the K point of the Brillouin zone assist inter-K valley scattering, which becomes observable in hBN if stacking faults provide a density of final electronic states [18]. In figure 4(b), we observe, in addition to the 5.9 eV line, a pronounced shoulder at 5.65 eV for growth temperatures of 1690, 1480, and 1390 °C, which corresponds to the first overtone arising from intervalley scattering assisted by the emission of one transverse optical phonon at the K point [18]. The observation of this component in the PL spectra in figure 4(b) indicates the presence of extended defects in hBN samples grown on HOPG, in agreement with AFM images in hBN on HOPG samples (figure 2) revealing the laterally polycrystalline hBN surface.

In contrast, for hBN samples grown on sapphire, AFM images of the hBN surface (figure 1) show that the hBN epilayers consist of nanocrystalline domains, so that extended defects cannot develop in this type of sample. The broad defect-related emission band below 5.7 eV can no longer be the superposition of many lines arising from both extended and point defects, as in high-quality hBN crystals [18]. For the samples grown on sapphire, the emission spectrum can only comprise the PL lines arising from point defects, i.e. the 5.27 and 5.56 eV lines, which were identified as being related to shallow transitions involving presumable boron-nitride divacancies [22]. We highlight here the striking similarity with hBN epilayers grown on sapphire by MOCVD where the PL spectrum also consists in two broad lines at 5.3 and 5.5 eV [21]. Whatever the MBE or MOCVD growth technique, these two lines have a larger width than in hBN crystals synthesized by the HTHP method [17]. This phenomenology indicates a larger inhomogeneous broadening, which may come from the sub-μm size of the hBN domains shown in figure 1 inducing drastic environment effects on the opto-electronic properties of point defects [23, 24]. In MOCVD, increasing the NH3 flow rate results in the suppression of the two broad lines at 5.3 and 5.5 eV, suggesting the importance of nitrogen vacancies in the formation of this specific defect [21]. This is also consistent with the residual p-type doping of hBN which favours nitrogen vacancies, in contrast to n-type AlN where the main vacancies originate from aluminium [25]. Theoretical calculations do not predict such shallow optical transitions for a N-vacancy [22] so another possibility needs to be considered. Among the few various configurations investigated by state-of-the-art calculations, the boron-nitride divacancy remains the most probable candidate [18].

4. Conclusion

High temperature MBE growth can produce hBN layers of high optical quality. hBN can be grown either on sapphire or highly oriented pyrolytic graphite, with superior optical properties in the deep ultraviolet in the latter case. The growth of hBN on highly oriented pyrolytic graphite is important for 2D device applications, and our results pave the way for a scalable fabrication of graphene-boron nitride van der Waals heterostructures and devices.

Acknowledgments

We gratefully acknowledge C L'Henoret for his technical support at the mechanics workshop. This work was financially supported by the network GaNeX (ANR-11-LABX-0014). GaNeX belongs to the publicly funded *Investissements d'Avenir* program managed by the French ANR agency. GC is a member of 'Institut Universitaire de France'. The MBE growth work is supported by the UK Engineering and Physical Sciences Research Council (EPSRC) grants EP/K040243/1, EP/L013908/1, EPSRC DTP grant EP/M50810X/1, and by the Leverhulme Trust (RPG-2014-129).

References

[1] Geim A K and Grigorieva I V 2013 *Nature* **499** 419
[2] Novoselov K S, Geim A K, Morozov S V, Jiang D, Zhang Y, Dubonos S V, Grigorieva I V and Firsov A A 2004 *Science* **306** 666
[3] Kobayashi Y, Kumakura K, Akasaka T and Makimoto T 2012 *Nature* **484** 223
[4] Majety S, Li J, Cao X K, Dahal R, Pantha B N, Lin J Y and Jiang H X 2012 *Appl. Phys. Lett.* **100** 061121
[5] Kneissl M and Rass J (ed) 2016 *III-Nitride Ultraviolet Emitters: Technology and Applications* (Berlin: Springer)
[6] Dahal R, Li J, Majety S, Pantha B N, Cao X K, Lin J Y and Jiang H X 2011 *Appl. Phys. Lett.* **98** 211110
[7] Li X, Sundaram S, Gmili Y E, Ayari T, Puybaret R, Patriarche G, Voss P L, Salvestrini J P and Ougazzaden A 2016 *Cryst. Growth Des.* **16** 3409
[8] Sutter P, Lahiri J, Albrecht P and Sutter E 2011 *ACS Nano.* **5** 7503
[9] Tay R Y, Griep M H, Mallick G, Tsang S H, Singh R S, Tumlin T, Teo E H T and Karna S P 2014 *Nano Lett.* **14** 839
[10] Tay R Y, Tsang S H, Loeblein M, Chow W L, Loh G C, Toh J W, Ang S L and Teo E H T 2015 *Appl. Phys. Lett.* **106** 101901
[11] Cassabois G, Valvin P and Gil B 2016 *Nat. Photon.* **10** 262
[12] Cheng T S *et al* 2016 *J. Vac. Sci. Technol.* B **34** 02L101
[13] Summerfield A *et al* 2016 *Sci. Rep.* **6** 22440
[14] Cho Y *et al* 2016 *Sci. Rep.* **6** 34474
[15] Elliott R J 1957 *Phys. Rev.* **108** 1384

[16] Museur L *et al* 2011 *Phys. Status Solidi* **5** 214–6
[17] Watanabe K and Taniguchi T 2004 *Nat. Mater.* **3** 404
[18] Cassabois G, Valvin P and Gil B 2016 *Phys. Rev.* B **93** 35207
[19] Schué L, Berini B, Betz A C, Plaçais B, Ducastelle F, Barjon J and Loiseau A 2016 *Nanoscale* **8** 6986
[20] Vuong T Q P, Cassabois G, Valvin P, Jacques V, Van Der Lee A, Zobelli A, Watanabe K, Taniguchi T and Gil B 2017 *2D Mater.* **4** 011004
[21] Du X Z, Li J, Lin J Y and Jiang H X 2016 *Appl. Phys. Lett.* **108** 052106
[22] Attaccalite C, Bockstedte M, Marini A, Rubio A and Wirtz L 2011 *Phys. Rev.* B **83** 144115
[23] Shen Y, Sweeney T M and Wang H 2008 *Phys. Rev.* B **77** 033201
[24] Jelezko F, Tietz C, Gruber A, Popa I, Nizovtsev A, Kilin S and Wrachtrup J 2001 *Single Mol.* **2** 255
[25] Stampfl C and Van de Walle C G 1998 *Appl. Phys. Lett.* **72** 459